

Disentangling electroweak effects in Z -boson production

S. CARRAZZA⁽¹⁾

⁽¹⁾ *Dipartimento di Fisica, Università di Milano & INFN, Sezione di Milano*

Summary. — Parton distributions with QED corrections open new scenarios for high precision physics. We recall the need for accurate and improved predictions which keeps into account higher order QCD corrections together with electroweak effects. We study predictions obtained with the improved Born approximation and the G_μ scheme by using two public codes: `DYNNLO` and `HORACE`. We focus our attention on the Drell-Yan Z -boson invariant mass distribution at low- and high-mass regions, recently measured by the ATLAS experiment and we estimate the impact of each component of the final prediction. We show that electroweak corrections are larger than PDF uncertainties for modern PDF sets and therefore such corrections are necessary to improve the extraction of future PDF sets.

PACS 12.15.Lk – Electroweak radiative corrections.

1. – Introduction

Recently the NNPDF Collaboration published sets of parton distribution functions with QED corrections, the so called NNPDF2.3QED sets [1-6]. These sets contain the photon PDF with its uncertainty determined for the first time from DIS and Drell-Yan LHC data.

In this work we estimate and compare to the PDF uncertainties the contributions to the invariant mass of the Drell-Yan Z -boson production due to electroweak corrections and the photon-induced channel, by considering the low-mass region, which is below the Z peak resonance and the high-mass tail.

In contrast to what was shown in Ref. [7] where predictions were computed with `FEWZ`, here we propose to combine two distinct parton level public codes: `DYNNLO` [8] for the NLO QCD prediction and `HORACE` [9] which provides the exact $\mathcal{O}(\alpha)$ electroweak radiative correction together with the photon-induced channel for the Z production. The motivation for this combination is the interest to measure the difference between predictions with electroweak effects at NLO/NNLO QCD accuracy computed in the improved Born approximation (IBA) instead of using electroweak correction computed by `FEWZ` in the G_μ scheme. The main difference between these choices is that effective couplings in the IBA reabsorb higher-order electroweak corrections and therefore it provides predictions in better agreement with experimental data.

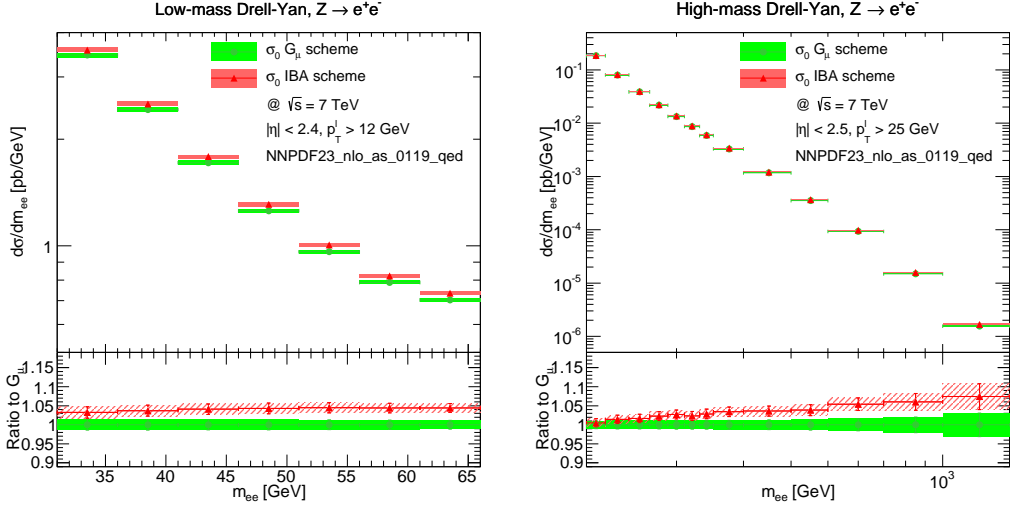


Fig. 1. – Born level predictions and respective ratios for low- (left) and high-mass (right) Drell-Yan, $Z \rightarrow e^+e^-$ production, using the IBA and the G_μ scheme. At low-mass there is a constant gap of 3-4% for all bins, while at high-mass, predictions increase progressively with the invariant mass, producing discrepancies of 7-8% in the last bin.

Computations are performed exclusively with the `NNPDF23_nlo_as_0119_qed` set of PDFs instead of using the respective LO and NNLO sets because here we will focus only on the NLO QCD accuracy and that is why we use a NLO set.

In the next sections, we first show the differences at Born level between the improved Born approximation (IBA), available in `HORACE` by default, and the G_μ scheme in `DYNNLO`, then, we proceed with the construction of the full prediction.

2. – Comparing the improved Born approximation (IBA) with the G_μ scheme

In order to obtain realistic results, which are ready for comparisons with real data, we have selected the kinematic range and cuts inspired by recent measurements performed by the ATLAS experiment for low- and high-mass Drell-Yan differential cross-section at $\sqrt{s} = 7$ TeV [10, 11].

Figure 1 shows the predicted distribution at Born level using the IBA (`HORACE`) and the G_μ scheme (`DYNNLO`) at low (left plot) and high (right plot) invariant mass regions, for the Drell-Yan process: $Z \rightarrow e^+e^-$. Here, the goal is to measure the numerical differences due to the choice of these methodologies.

For all distributions, the Monte Carlo uncertainty is below the percent level. We have computed predictions with the `NNPDF23_nlo_as_0119_qed` set of PDFs because this is the set that we use to build the complete prediction at NLO in QCD with electroweak effects. The uncertainties shown in the figure have been calculated as the $1\text{-}\sigma$ interval obtained after averaging over the 100 replicas provided by this set.

In the low-mass region, we have applied kinematic cuts to the lepton pair imposing: $p_T^l > 12$ GeV and $|\eta^l| < 2.4$ as in ATLAS [10]. In this region we observe an almost flat gap of 3-4% between the IBA and G_μ predictions, however in the bin $m_{ee} = 51 - 56$ GeV the difference is slightly higher.

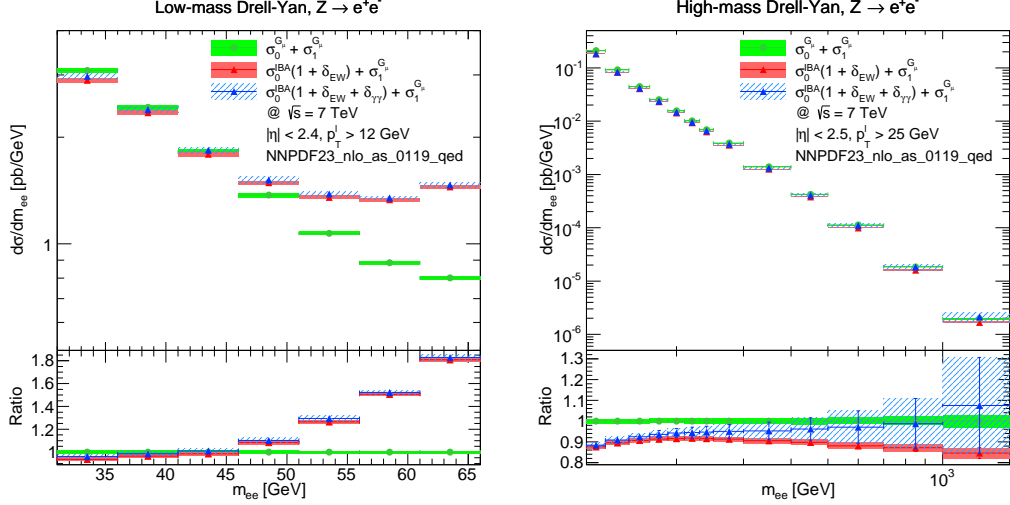


Fig. 2. – Comparison of predictions and respective ratios for low- (left) and high-mass (right) Drell-Yan, $Z \rightarrow e^+e^-$ production. We compare the NLO QCD prediction provided by DYNLLO (green distribution) with: the combined prediction with δ_{EW} (red distribution) and with the $\delta_{EW} + \delta_{\gamma\gamma}$ (blue distribution).

On the other hand, in the high-mass region we have applied the following kinematic cuts: $p_T^l > 25$ GeV and $|\eta^l| < 2.5$ as in Ref. [11]. We observe a progressive increase of the central value prediction as a function of the invariant mass, reaching a maximum of 7-8% at the highest bin in m_{ee} . This suggests that the running of $\alpha(Q^2)$ in the IBA can play a crucial role when determining with accuracy the predictions in such region.

It is important to highlight that in both cases, PDF uncertainties are smaller than the observed differences induced by the choice of the scheme. These results are fully consistent with the IBA implementation discussed in Ref. [9]. In the sequel we are interested in combining electroweak effects with higher order QCD corrections in the IBA and then compare these results to pure QCD G_μ predictions.

3. – Disentangling electroweak effects

At this point, we are interested in building a prediction based on IBA which includes NLO QCD with $\mathcal{O}(\alpha)$ correction and the photon-induced channel. We propose to extract the NLO correction from DYNLLO by removing its Born level, which contains the direct and strong dependence on the G_μ scheme, and combine the result with the HORACE prediction. Schematically this can be achieved by defining the quantities:

$$(1) \quad \sigma_{\text{DYNLLO}} = \sigma_0^{G_\mu} + \sigma_1^{G_\mu},$$

$$(2) \quad \sigma_{\text{HORACE}} = \sigma_0^{\text{IBA}}(1 + \delta_{EW} + \delta_{\gamma\gamma}),$$

where σ_0^{IBA} and $\sigma_0^{G_\mu}$ are the Born levels presented in Figure 1, $\sigma_1^{G_\mu}$ the NLO QCD, δ_{EW} the $\mathcal{O}(\alpha)$ electroweak correction and $\delta_{\gamma\gamma}$ the photon-induced contribution.

The combination is then constructed in the following way:

$$\begin{aligned}
 (3) \quad \sigma_{\text{Total}} &= \sigma_{\text{DYNL0}} + \sigma_{\text{HORACE}} - \sigma_0^{G_\mu} \\
 (4) \quad &= \sigma_0^{\text{IBA}} + \sigma_0^{\text{IBA}} \delta_{\text{EW}} + \sigma_0^{\text{IBA}} \delta_{\gamma\gamma} + \sigma_1^{G_\mu}.
 \end{aligned}$$

where we remove the DYNL0 Born level while we include the NLO QCD correction in the final prediction.

We are aware that using this methodology we improve the combination but we do not remove entirely the pure G_μ dependence at higher orders, however this is the best combination we can propose without applying technical modifications to both codes ⁽¹⁾.

In Figure 2 we compare σ_{DYNL0} with σ_{Total} , the combination presented in Eq. 4, with and without the $\delta_{\gamma\gamma}$ term. For all distributions we compute the 1- σ uncertainty except when including the photon-induced channel where we have used the 68% c.l. as in Ref. [1].

In the low-mass region the inclusion of $\mathcal{O}(\alpha)$ electroweak corrections has a strong impact on the last four bins, where differences can reach $\sim 80\%$ in comparison to the pure NLO QCD G_μ prediction, while the same correction for the high-mass distribution shows a moderate impact which is below $\sim 20\%$ for the highest invariant mass bin. This behavior is expected and derives from the shape of the Z -boson invariant mass: bins located in a region lower than the Z peak resonance undergoes large positive corrections while at high invariant mass we observe a change of sign of such corrections. It is important to highlight that modern data provided by the LHC experiments are already corrected by final-state photon radiation which carries a dominant fraction of the electroweak effects shown in Figure 2.

The photon-induced contribution has a moderate impact in the low-mass region while for high-mass it is dominant: this behavior is expected and due to the presence of the Z peak resonance where the photon-induced channel is negligible.

Also from these plots of Figure 2, it is important to emphasize again that modern PDF sets, as the NNPDF2.3QED, have uncertainties which are accurate enough to appreciate the differences due to scheme choices and electroweak effects, including the new photon PDF, which shows a stable behavior of uncertainties in all invariant mass regions except at very high-mass bins where uncertainties grow, reaching more than $\sim 20\%$. This situation will be improved in future by including more relevant and precise data to constrain the photon PDF.

4. – Outlook

We have shown that the choice of the coupling scheme clearly modifies the predictions when looking at realistic experimental regions for the Z -boson production. We have constructed a combined prediction which includes the $\mathcal{O}(\alpha)$ electroweak corrections together with the photon-induced channel in the IBA using public codes. We show that uncertainties from modern PDF sets are smaller than electroweak effects and therefore such corrections will provide noticeable differences when extracting future PDF sets.

Finally, in a future work we expect to provide a similar study for other processes and kinematic regions, by propagating consistently the IBA to higher orders and producing a direct comparison to the FEWZ results.

⁽¹⁾ In preparation by S.C., G. Ferrera, A. Vicini.

REFERENCES

- [1] R. D. Ball *et al.* [NNPDF Collaboration], Nucl. Phys. B **877** (2013) 2, 290 [arXiv:1308.0598 [hep-ph]].
- [2] V. Bertone, S. Carrazza and J. Rojo, arXiv:1310.1394 [hep-ph].
- [3] S. Carrazza [NNPDF Collaboration], arXiv:1305.4179 [hep-ph].
- [4] S. Carrazza [NNPDF Collaboration], PoS DIS **2013** (2013) 279 [arXiv:1307.1131 [hep-ph]].
- [5] S. Carrazza, S. Forte and J. Rojo, arXiv:1311.5887 [hep-ph].
- [6] P. Skands, S. Carrazza and J. Rojo, arXiv:1404.5630 [hep-ph].
- [7] R. Boughezal, Y. Li and F. Petriello, Phys. Rev. D **89** (2014) 034030 [arXiv:1312.3972 [hep-ph]].
- [8] S. Catani and M. Grazzini, Phys. Rev. Lett. **98** (2007) 222002 [hep-ph/0703012].
- [9] C. M. Carloni Calame, G. Montagna, O. Nicrosini and A. Vicini, JHEP **0710** (2007) 109 [arXiv:0710.1722 [hep-ph]].
- [10] G. Aad *et al.* [ATLAS Collaboration], arXiv:1404.1212 [hep-ex].
- [11] G. Aad *et al.* [ATLAS Collaboration], Phys. Lett. B **725** (2013) 223 [arXiv:1305.4192 [hep-ex]].